

# High sensitivity microcrack hydroxylated MWCNTs/ ecoflex composite flexible strain sensor based on proton irradiation engineering

Xiaoqing Yue<sup>1</sup>, Jianqun Yang<sup>1</sup>, Lei Dong<sup>1</sup>, Xuwen Wang<sup>2</sup>, Yuhang Jing<sup>3</sup>, Weiqi Li<sup>4</sup>, Xingji Li<sup>1\*</sup>

<sup>1</sup>School of Materials Science and Engineering, Harbin Institute of Technology, Harbin, China

<sup>2</sup>Institute of Flexible Electronics, Northwestern Polytechnical University, Xi'an, China

<sup>3</sup>School of Astronautics, Harbin Institute of Technology, Harbin, China

<sup>4</sup> School of Physics, Harbin Institute of Technology, Harbin, China

\*To whom correspondence should be addressed. E-mail: lxj0218@hit.edu.cn (X. J. Li)

## SUPPORTING INFORMATION

Table

**Table S1** Changes of hydroxylated MWCNTs  $sp^2/sp^3$  after proton irradiation.

Fluence( $e/cm^2$ )	0	$1 \times 10^{12}$	$5 \times 10^{12}$	$1 \times 10^{13}$	$1 \times 10^{14}$
$sp^2/sp^3$	5.60	4.79	4.47	4.38	3.40

Figure

**Figure S1** Raman of hydroxylated MWCNTs after proton irradiation.

**Figure S2** Raman of hydroxylated MWCNTs after electron irradiation.

**Figure S3** XPS of hydroxylated MWCNTs after proton irradiation.

**Figure S4** XPS of hydroxylated MWCNTs after electron irradiation.

**Figure S5** FTIR of hydroxylated MWCNTs after proton irradiation.

**Figure S6** FTIR of hydroxylated MWCNTs after electron irradiation.

**Figure S7** The peak fitting results of Si2p high-resolution XPS binding energy spectrum of flexible substrate before and after irradiation.

**Figure S8** The sensing performance of sensors under different strain rates.

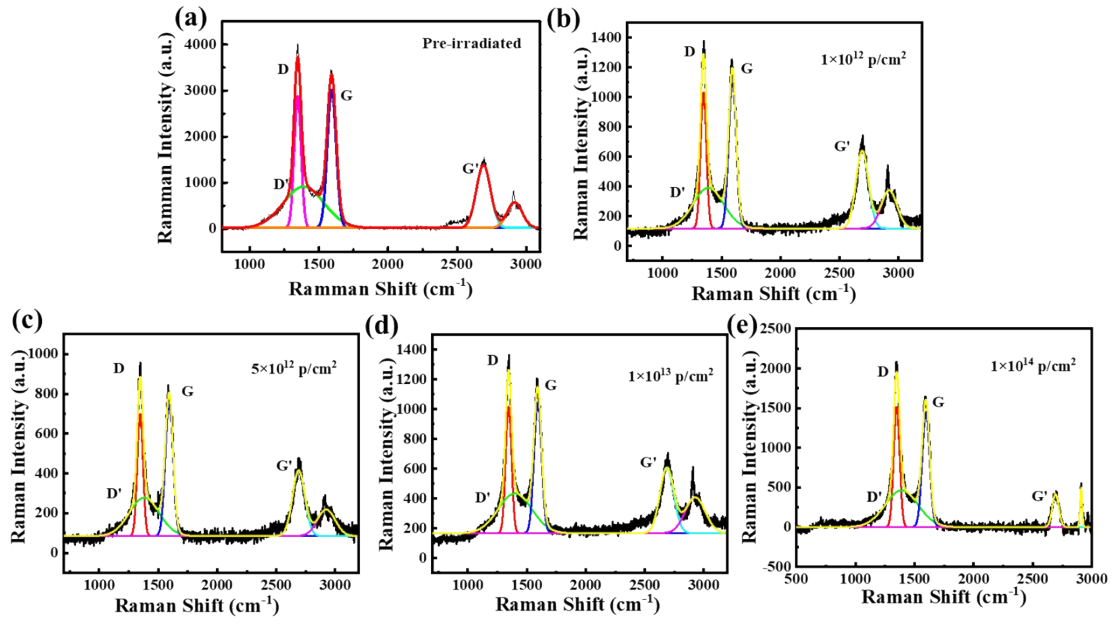


Figure S1

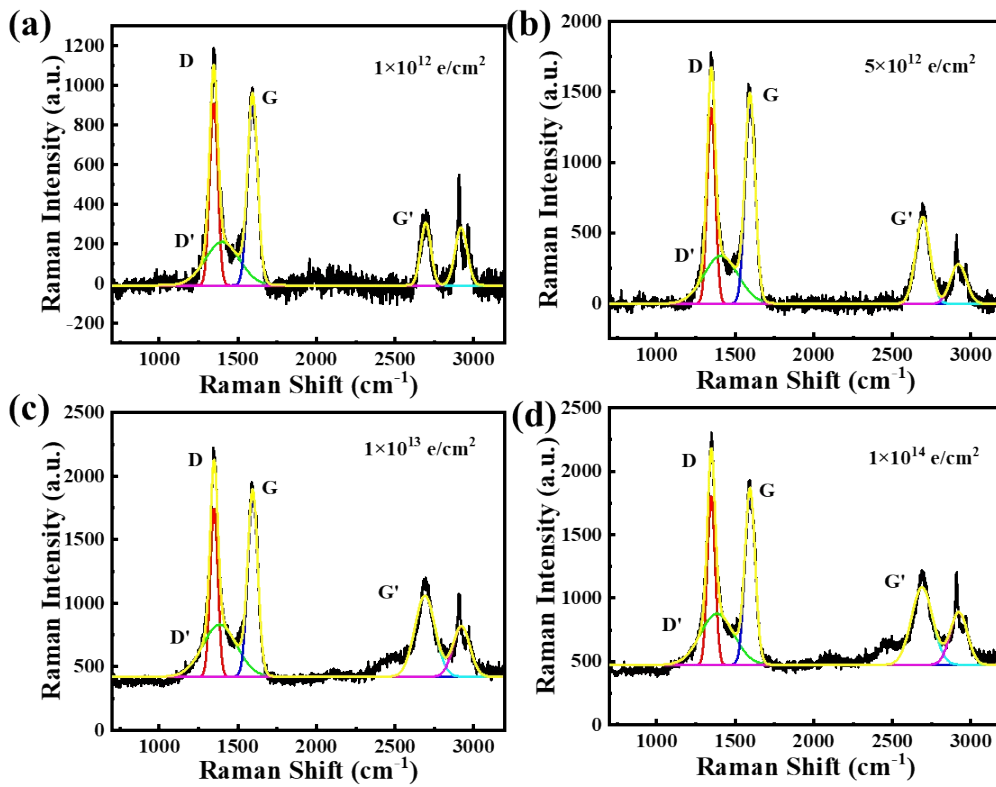


Figure S2

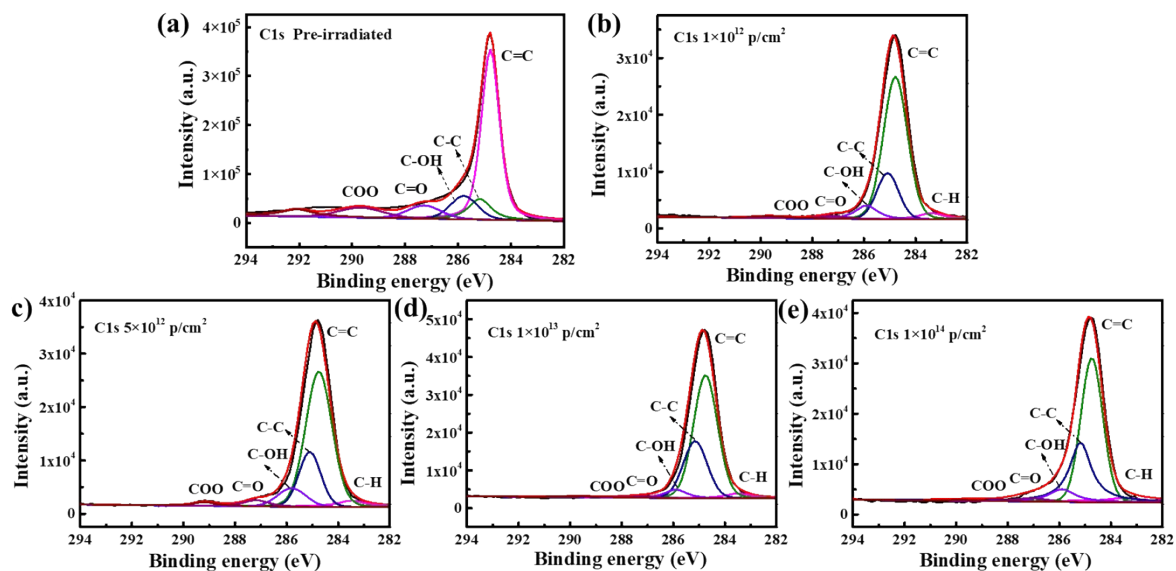


Figure S3

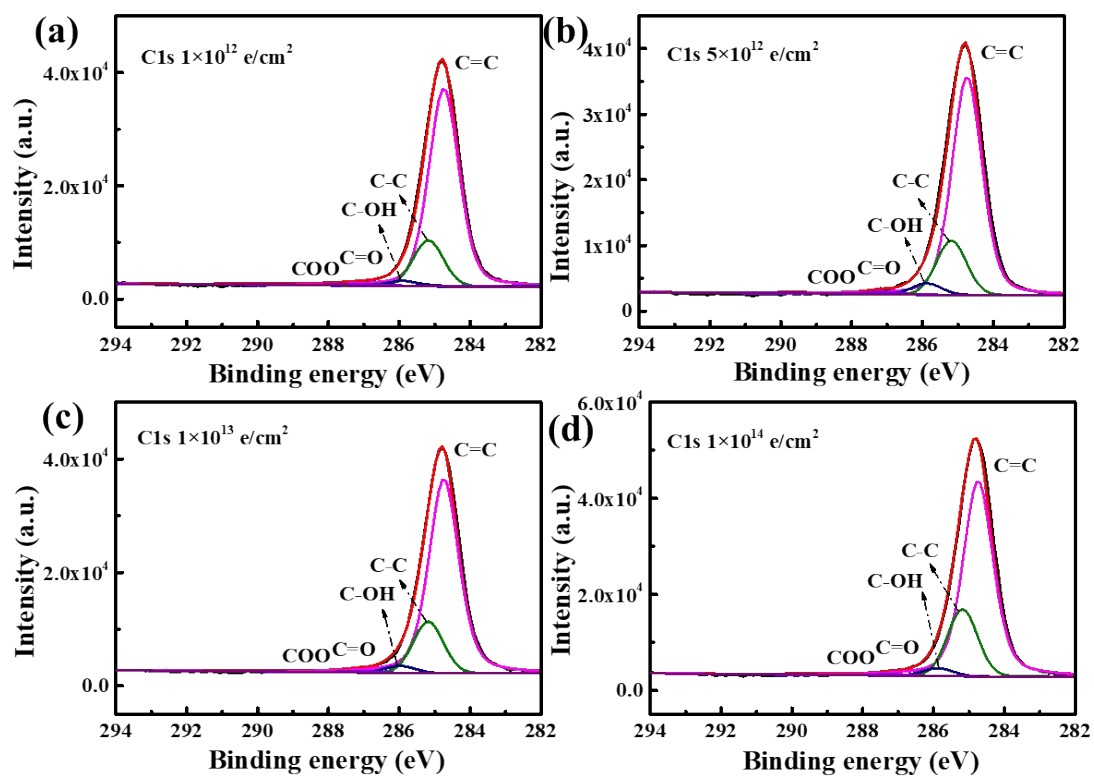


Figure S4

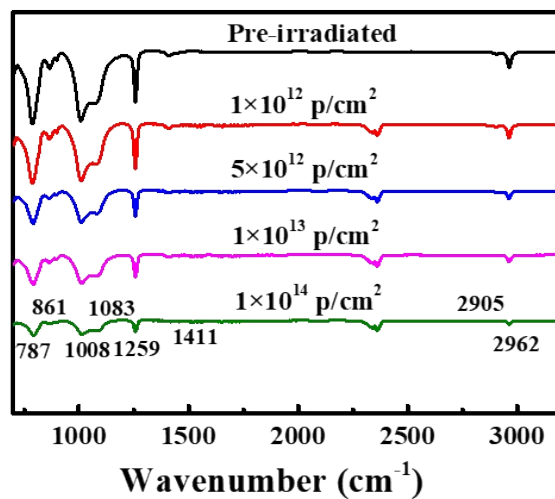


Figure S5

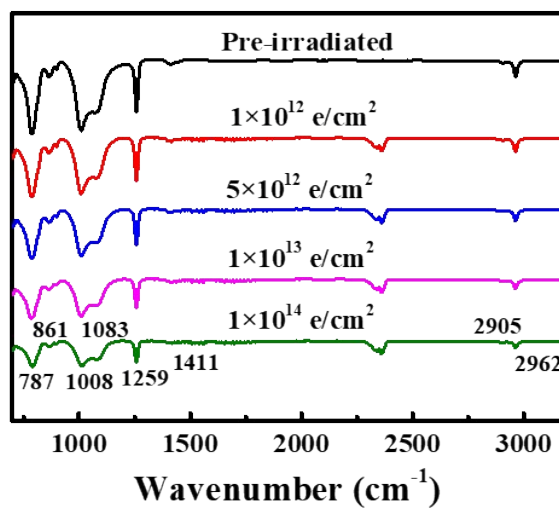


Figure S6

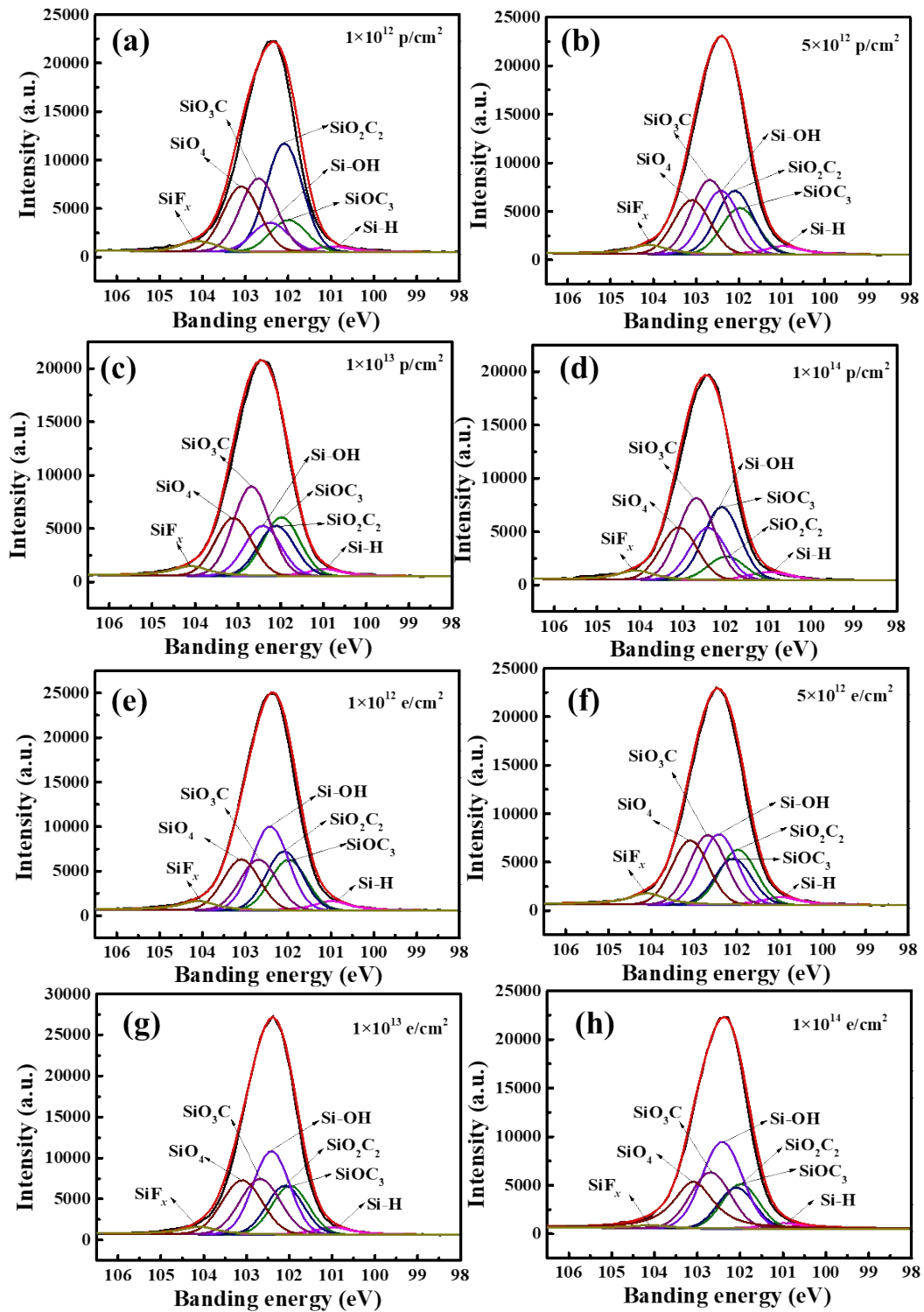


Figure S7

XPS data can be processed by XPSPEAK software, and then the binding energy peaks of different functional groups can be obtained. The contents of different functional groups were obtained by integrating the binding energy peaks of different functional groups.

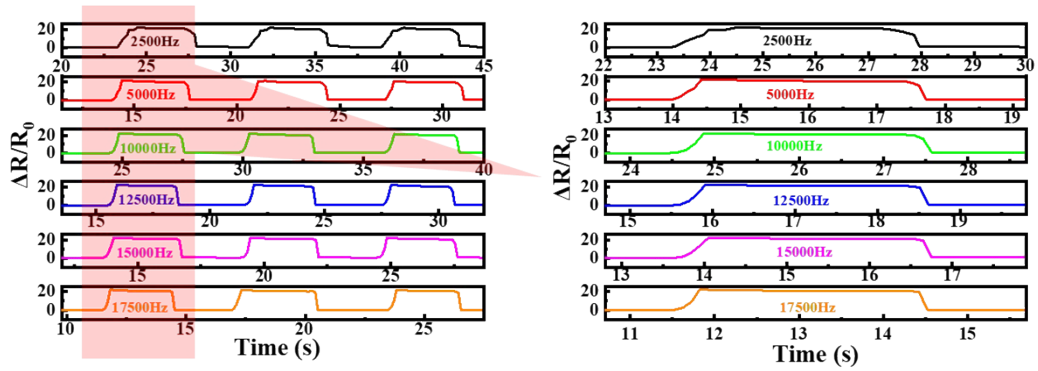


Figure S8

Figure S8 shows the sensing performance of the sensor under different strain rates. Among them, 2500 Hz, 5000 Hz, 1000 Hz, 12500 Hz, 15000 Hz and 17500 Hz, respectively corresponding to 6.25 mm/s, 12.5 mm/s, 25 mm/s, 31.25 mm/s, 37.5 mm/s and 43.75 mm/s. It can be seen from the figure that the responsiveness of the sensor is consistent under different strain rates. However, the change curve of the sensor is unstable at low strain rate. Therefore, it is not advisable to choose a low strain rate during the testing process.